Color Spaces in Data Fusion of Multi-temporal Images

Roberta Ferretti(✉) and Silvana Dellepiane

Università degli Studi di Genova, DITEN, via Opera Pia 11a 16145, Genova, Italy
roberta.ferretti@edu.unige.it, silvana.dellepiane@unige.it

Abstract. The data fusion process is strongly recommended in biomedical applications. It allows a better detection and localization of the pathology, as well as the diagnosis and follow-up of many diseases [1], especially with multi-parametric or multi-temporal data.

The independent visualization of multiple images from large volumes is a main cause of errors and inaccuracy within the interpretation process. In this respect, the use of color fusion methods allows to highlight small details from multi-temporal and multi-parametric images.

In the present work, a color data fusion approach is proposed for multi-temporal images, in particular for images of the liver acquired through triphasic CT.

The best color association has been studied considering various data sources. Different metrics for quality assessment have been selected from the color space theory, making an interesting comparison with the human visual perception.

Keywords: Data fusion · Color · Triphasic

1 Introduction

The Data fusion technique combines data from two or more sources within a single piece of information having a high informative content. The aim of image fusion is to integrate individual two-dimensional images, three-dimensional images (volumes or video sequences), or images with larger dimensions, in order to improve visual perception, reduce uncertainty and redundancy of information and maximize the probability of localizing relevant information [2]. In this way, a broader spatial and temporal coverage, a greater reliability and a considerable reduction in the amount of data to be displayed are obtained, without significantly affecting the amount of relevant information [2].

In the medical field, image fusion simplifies the assessment of spatial relationships between images displayed side by side [3]. In this respect, it is important to consider that identical shapes and lines may appear in different sizes, depending on background shades and colors [2]. The data fusion technique is not widely used, but it can make a quantitative assessment of the images easier and help physicians to deliver an impartial and objective diagnosis in a short amount of time. Furthermore, being able to realize multi-sensor, multi-parametric and multi-temporal fusions, allows the physician to analyze different types of images with a different information content.

V. Murino and E. Puppo (Eds.): ICIAP 2015, Part I, LNCS 9279, pp. 612–622, 2015.
DOI: 10.1007/978-3-319-23231-7_55

In image fusion, the information content is displayed in a single image, often revealing particulars that are otherwise invisible to the human eye [4].

In the medical field, the employment of image fusion during the last twenty years has promoted the research and study of new techniques or the adoption of existing techniques in new application fields [4]. A key feature in data fusion process is the analysis and the possibility of correlating the content of the original images. The relevant information content of each source can be stored and then combined to form a new image.

By analyzing a specific case study of liver tumor, this work aims to:

- find a rule capable of associating RGB channels to the images, in order to highlight the image content at the best;
- show how human visual perception is often misleading and can cause interpretation errors;
- improve the localization and identification of the pathology, characterizing significantly the nature of a lesion.

Starting from a data fusion based on RGB color representation we have tried to demonstrate how results can be enhanced as regards information.

The aim of the proposed work is not to obtain a classification, but to improve image display and show how image details can be immediately highlighted using colors.

In the following paragraph, we analyze different color spaces and metrics necessary to evaluate the results of the color data fusion.

2 Color Space and Metrics

In literature several color spaces and metrics have been proposed, all aimed at representing color in different contexts, and evaluating the similarity between two colors in the view of the human visual perception [5].

2.1 Color Space

Digital color images are usually represented in the RGB space. However, RGB does not represent a perceptually uniform color space; this means that the color difference calculated in this space (for example, using the Euclidean distance) does not correspond to that perceived by the human eye [6]. To overcome this problem the International Committee on Colorimetry, CIE (Commission Internationale de l'Eclairage), has defined the two color spaces L*a*b* and L*u*v*[6], where color components are separated from the Luminance information. However, even though performing better than RGB space, these color spaces are not so perceptually homogeneous, as they are claimed to be. These two representations are determined through an intermediate reference space, referred to as CIE XYZ, which is derived from RGB space using the following linear transformation [7, 8].

$$\begin{bmatrix} X \\ Y \\ Z \end{bmatrix} = \begin{bmatrix} 0.4887180 & 0.3106803 & 0.2006017 \\ 0.1762044 & 0.8129847 & 0.0108109 \\ 0.0000000 & 0.0102048 & 0.9897952 \end{bmatrix} \cdot \begin{bmatrix} R \\ G \\ B \end{bmatrix} \tag{1}$$

L*a*b* and L*u*v* [7, 8] are defined by the following non-linear transformations. The L*a*b* formulae are:

$$L = 116 f\left(\frac{Y}{Y_n}\right) - 16$$

$$a^* = 500\left[f\left(\frac{X}{X_n}\right) - f\left(\frac{Y}{Y_n}\right)\right]$$

$$b^* = 200\left[f\left(\frac{Y}{Y_n}\right) - f\left(\frac{Z}{Z_n}\right)\right] \tag{2}$$

where:

$$f(q) = \begin{cases} q^{1/3}, & if\ q > 0.008856 \\ 0.787q + 16.116, & otherwise \end{cases}$$

The L*u*v* formulae are:

$$L^* = \begin{cases} 116\sqrt[3]{y_n} - 16 & y_n > \varepsilon \\ k y_n & y_n \le \varepsilon \end{cases}$$

$$u^* = 13L^*(u' - u'_n)$$

$$v^* = 13L^*(v' - v'_n) \tag{3}$$

where:

$$y_n = {Y}/{Y_n}, \qquad \varepsilon = 0.008856, \quad k = 903.3$$

$$u' = \frac{4X}{X+15Y+3Z}, \qquad v' = \frac{9Y}{X+15Y+3Z}$$

$$u'_n = \frac{4X_n}{X_n+15Y_n+3Z_n}, \quad v'_n = \frac{9Y_n}{X_n+15Y_n+3Z_n}$$

For both formulae X_n, Y_n and Z_n are the reference white defined by a CIE standard illuminant, E [6], in this case.

2.2 Color Metrics

Various measures are used to calculate the difference between two colors, all developed to better reflect human perception without confusing different colors and without separating similar colors [5]. Several metrics have been created over time, because none of them seems to fully satisfy this goal.

The most relevant are briefly described as follows. They have also been used in the proposed approach.

Euclidean Distance. The Euclidean distance is frequently employed in RGB and L*a*b* spaces, see the equation (4) and (5) [9]:

$$\Delta \mathrm{E}_{RGB} = \sqrt{(R_1 - R_2)^2 + (G_1 - G_2)^2 + (B_1 - B_2)^2} \tag{4}$$

$$\Delta E^*_{ab} = \sqrt{(L^*_1 - L^*_2)^2 + (a^*_1 - a^*_2)^2 + (b^*_1 - b^*_2)^2} \tag{5}$$

CMC. The Color Measurement Committee (CMC) of the Society of Dyers and Colorists [9] defined a color difference metric called CMC (*l*:*c*) based on the CIE L*a*b*. $\Delta L^*, \Delta C^*_{ab}$, and ΔH^*_{ab} are, respectively, lightness, chroma, and hue difference. The parameters l and c are, respectively, lightness weighting, and chroma weighting. Then:

$$\Delta E^*_{CMC(l:c)} = \sqrt{\left(\frac{\Delta L^*}{l S_L}\right)^2 + \left(\frac{\Delta C^*_{ab}}{c S_C}\right)^2 + \left(\frac{\Delta H^*_{ab}}{S_H}\right)^2} \tag{6}$$

where:

$$S_L = \begin{cases} 0.511 & L^*_1 < 16 \\ \dfrac{0.040975 L^*_1}{1 + 0.01765 L^*_1} & L^*_1 \geq 16 \end{cases}$$

$$S_C = \frac{0.0638 C^*_1}{1 + 0.0131 C^*_1} + 0.638\,, \quad S_H = S_C(FT + 1 - F) \quad , \quad F = \sqrt{\frac{{C^*_1}^4}{{C^*_1}^4 + 1900}}$$

$$T = \begin{cases} 0.56 + |0.2 \cos(h_1 + 168°)| & 164° \leq h_1 \leq 345° \\ 0.36 + |0.4 \cos(h_1 + 35°)| & otherwise \end{cases}$$

The terms S_L, S_C, and S_H are the weighting functions for the lightness, chroma, and hue components, respectively. Except for textile industry, it is usually recommended that l=2 and c=1.

CIEDE2000. The CIE has proposed another formula: CIEDE2000 [10]. which should be able to assess small color differences.. Here we have:

$$\Delta E^*_{00} = \sqrt{\left(\frac{\Delta L'}{k_L S_L}\right)^2 + \left(\frac{\Delta C'}{k_C S_C}\right)^2 + \left(\frac{\Delta H'}{k_H S_H}\right)^2 + R_T \frac{\Delta C'}{k_C S_C} \frac{\Delta H'}{k_H S_H}} \tag{7}$$

where:

$$S_L = 1 + \frac{0.015(\bar{L} - 50)^2}{\sqrt{20 + (\bar{L} - 50)^2}}, \quad S_C = 1 + 0.045 \bar{C}', \quad S_H = 1 + 0.015 \bar{C}' T$$

$$\Delta L' = L^*_1 - L^*_2, \qquad \Delta C' = C'_1 - C'_2, \qquad \Delta H' = 2\sqrt{C'_1 C'_2} \sin\left(\frac{\Delta h'}{2}\right)$$

$$T = 1 - 0.17\cos(\bar{H}' - 30°) + 0.24\cos(2\bar{H}') + 0.32\cos(3\bar{H}' + 6°)\, 0.2\cos(4\bar{H}' - 63°)$$

$$R_T = -2\sqrt{\frac{\bar{C}'^7}{\bar{C}'^7 + 25^7}}\sin 60° \left[\exp\left(-\left[\frac{\bar{H}' - 275°}{25°}\right]^2\right)\right]$$

3 The Proposed Method

This work applies a data fusion approach based on the use of color within an innovative multi-parametric diagnostic method: triphasic CT of the liver.

3.1 Triphasic CT of the Liver

This technique is based on the acquisition of three volumes, upon the injection of a contrast agent; the first volume is the arterial phase, the second one is the portal venous phase, and the last one is the delayed phase. These acquisitions are performed respectively after 20-30 seconds, 60-70 s, and 60-180 s from the contrast material injection [11, 12].

The 75-100% of potential types of liver tumors receives blood from the hepatic artery: they are known as hypervascular tumors. Neoplasms are hypovascular tumors and represent about 25% of all tumors [11]. The venous phase is more sensitive for the detection of lesions, while the arterial and delayed phases can provide additional information on the vascularity of lesions in order to clarify their nature [13]. The combination of the arterial and venous phases reveals 92% of the lesions, the combination of the arterial and delayed phases detects 91% of the lesions, and the combination of the venous and delayed phases accounts for 80% of the lesions. The combination of all three phases detects 92% of the lesions [14].

3.2 Color Fusion

The scientific literature describes many methods for the registration phase, that is the phase preceding the actual data fusion process, but very little has been formally said about the combination of the original data, their information content, and the fusion of multi-temporal and multi-parameter information [15, 16].

The algorithm proposed in this paper should allow the fusion of images by the use of color. In a different way with respect to the classical Look-Up–Table method, the proposed process envisions the generation of an actual color image. To this end, it is necessary to specify the content of the three channels of a color image, i.e., the Red, Green and Blue channels.

Starting from the original CT phase images, a visual enhancement of their global content should be achieved through the display of a most informative color image.

In this respect, it is necessary to perform an accurate and adaptive choice of the criteria to decide which image is to be associated to each color channel RGB. In the literature, this is a novel approach since, usually, the choice of the associations is random.

To this end, a quantitative study has been carried out along with a qualitative analysis. Appropriate objective measurements have been investigated in order to evaluate the best result from among the various possibilities offered by the given data fusion procedure.

Fig.1 shows the structure of the proposed algorithm.

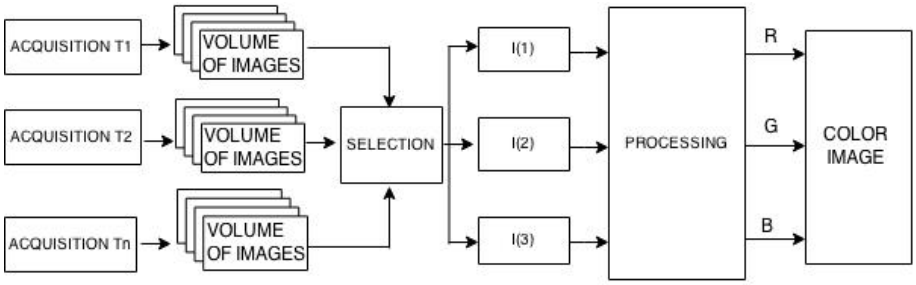

Fig. 1. Description of the algorithm fusion

The first step of the algorithm is aimed at identifying the images to be used as input to the fusion process. This is necessary in order to localize the images containing the area of interest and select them accurately in all three phases. In fact, the three volumes acquired may not have a direct correspondence between homologous slices.

The association of a color channel with a specific image may refer to the original images (8), or to new images (9) obtained from some processing algorithm applied to them. For instance, simple operators such as subtraction or average can be applied. In previous works other linear transformations were proposed, such as those derived from the PCA application [17].

$$\begin{cases} R = I(i) \\ G = I(j) \\ B = I(k) \end{cases} \quad with\ i,j,k = 1,2,3\ and\ i \neq j \neq k \tag{8}$$

$$\begin{cases} R = f_R(I(i), I(j), I(k)) \\ G = f_G\big(I(i), I(j), I(k)\big) \\ B = f_B(I(i), I(j), I(k)) \end{cases} \tag{9}$$

Once images to be used as input to the data-fusion process have been chosen, it is necessary to establish the most appropriate association with the RGB channels.

For every three images provided as input to the algorithm, it is possible to make different permutations between the RGB channels, and then get different results. Permutation of RGB channels is N!=6; this causes significant changes in the final visualization result. A study on synthetic images has been carried out in order to optimize this stage, provide the best possible result and define the rules of color association to the original images. The results have been evaluated using the metrics: ΔE^*_{RGB}, ΔE^*_{ab}, ΔE^*_{uv}, $\Delta E^*_{CMC(l:c)}$, and ΔE^*_{00}, as described above.

Then, qualitative and quantitative assessments have been conducted a posteriori also on the CT final images. The aim was to select the final image with the highest

informative content from a perceptual point of view and check if the results obtained on synthetic images were verified.

All the resulting images have been submitted to several experts for a quantitative assessment. According to it, none of the distances totally reflects human judgment.

4 Experimental Results

Before applying the color data fusion on CT images, we created synthetic images in order to understand how the results could change by varying the association image/RGB channel. There are three images with three different backgrounds: white, gray and black. The background of each image displays colored numbers (white, gray and black), in order to consider all possible combinations background/colored numbers. This is necessary to obtain all permutations once applied the color data fusion.

After a visual and analytical study supported by the use of distances between colors on the different images obtained, we can state that, if the detail we want to highlight appears exclusively in one of the input images, it is advisable to associate that image to the red, or better, to the green channel. This is because the eye, under the same luminous intensity, is more sensitive to green than to red and blue lights.

Then a color data fusion approach is applied to images of the triphasic liver in order to better localize and identify the disease, as well as to significantly characterize the nature of a lesion.

To this purpose, a direct color fusion algorithm has been applied in order to compare human visual perception to the actual image information content. This new approach makes use of a maximum contrast criterion and suggests a practical rule to enhance the visualization.

The proposed algorithm has been applied to a case study regarding a Hepatocellular carcinoma (HCC) tumor after chemoembolization. In the case illustrated in Fig.2 the presence of a known sign in S8/S4 liver segments (45x33x48mm) should be underlined. Such a formation has an inhomogeneous appearance as it is characterized in part by necrotic hypodense tissue and in part by neoplastic persistent tissue, as shown respectively with the arrows in Fig. 2a. The former is free of contrastographic enhancement. The latter shows some strengthening in arterial phase and moderate washout, as compared to neighboring parenchyma in venous and delayed phases.

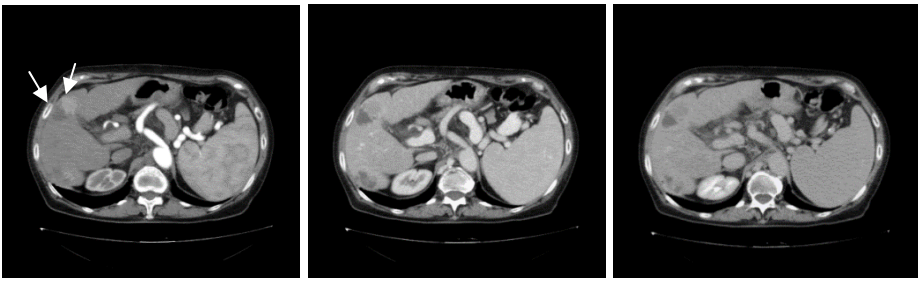

(a) (b) (c)

Fig. 2. Images of triphasic CT: (a) arterial phase, (b) venous phase, (c) delayed phase

Some general pre-processing steps have been applied to all the images of the tri-phasic volumes, as regards calibration, filtering and masking. The images are not perfectly registered to one another, but it is not the aim of this paper to propose a method of registration or pause on this aspect.

When visually analyzing the case, shown in Fig.2, a human expert perceives the neoplastic tissue to be lighter in the arterial phase as compared with the venous and the delayed phases. The necrotic tissue in all three phases is darker than the tumor and the liver; but also in this case it appears brighter in the arterial phase than in the other two phases.

A color fusion of the three phases is proposed using the association image/channel RGB of the formula (8) to test whether the perception is in line with the actual image content. Performing a direct association of each RGB channel with one of the original CT phases, as shown in Fig.3, it is possible to appreciate how the tumor and the necrotic tissue Hounsfield Units (HU) are not changing between phases. This can be observed by the small presence of color in the tumor and in the necrotic tissue.

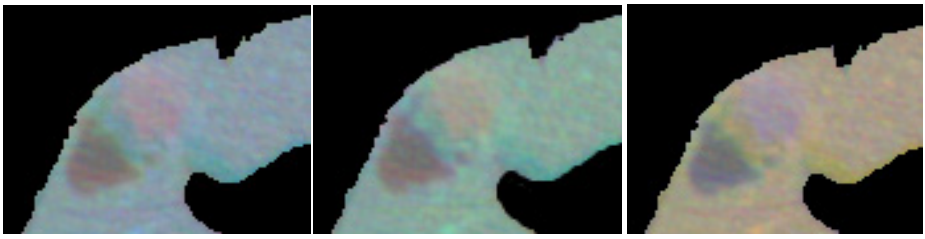

(a) (b) (c)

Fig. 3. RGB fusion of three phases with different permutation.

In order to highlight the pathology with respect to healthy tissue, images have been processed to each other using different algorithms. The most satisfactory result has been obtained by subtracting the phases, while the best combination is represented by the Difference-Image between arterial and delayed phases, where the tumor-to-parenchyma contrast is maximum (10).

$$\begin{cases} f_m = I(1) \\ f_n = I(3) \\ f_l = I(1) - I(3) \end{cases} \tag{10}$$

All the associations between arterial, delayed, and difference images have been performed; in Fig.4, some examples are shown. As may be seen, the color allows the tumor to stand out from the parenchyma.

All results, obtained by permutation of the direct fusion of original images and processed images, have been assessed visually and with appropriate color distance metrics. This allowed studying the results and defining the best combination.

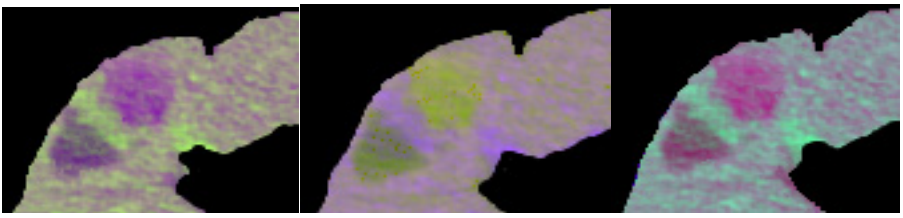

(a) (b) (c)

Fig. 4. RGB fusion of arterial phase, delayed phase and difference image between them with different permutation

The data in Fig.5 show the correlation between the results obtained from human perception and those achieved with the application of different color metrics. In particular, the abscissa axis reports the ratings from 1 to 13 (from worst to best) suggested by a sample of people who visually evaluated the images. Fig.3 shows the three worst images and Fig.4 the three best ones. On the ordinates, we can find the results from the different distances calculated, where a small result corresponds to very similar colors.

Looking at the graph it is possible to observe that not all metrics applied show the same results. The distance ΔE_{RGB} does not cause variations among the three worst and the three best results, and provides the same result starting from different colors comparisons. Another distance that does not meet the requirements is the ΔE^*_{00}. In this case, the distinction between worst and best results is not clear, and in fact, the results in both cases are very similar.

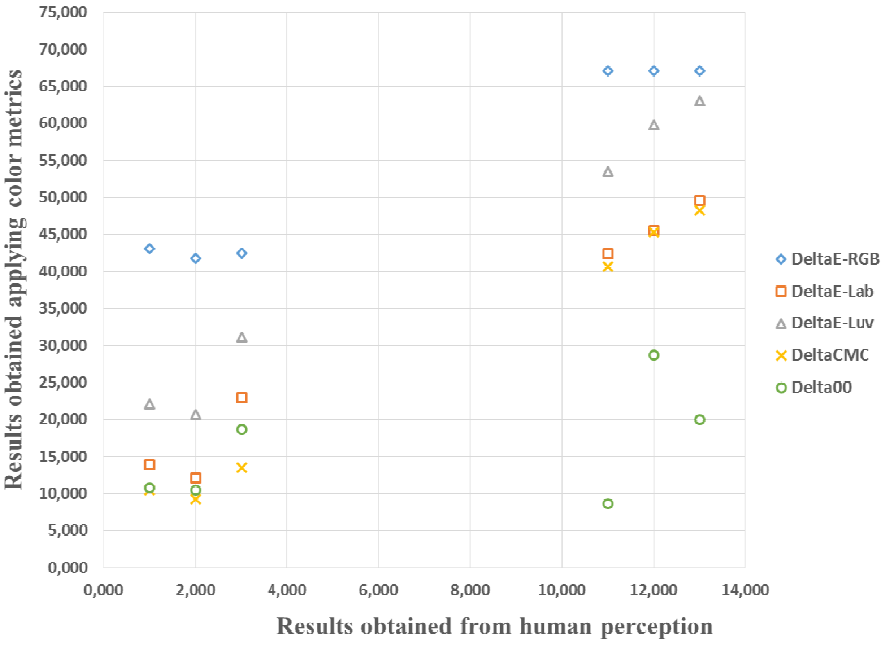

Fig. 5. Graph of the correlation.

Comparing the results obtained with the calculation of the most promising distances, we can see that in all three cases, (ΔE^*_{ab}, ΔE^*_{uv} and $\Delta E^*_{CMC(l:c)}$) there is a gap between the results considered perceptually the worst (bottom left corner) and the best (top right corner). The best results in all three cases fully reflect the results perceived by the human eye. Considering the worst results, no one of them fully reflects the order relevant to human perception, but the one that comes the closest is the $\Delta E^*_{CMC(l:c)}$.

Two of the three best results obtained visually and by a quantitative measure show in the green channel the image with the highest information content. This confirms the results previously achieved on synthetic images. The best image is shown in Fig.4a with the combination of delayed phase, difference image and arterial phase in association with RGB, respectively.

As compared with PCA-transform-based data fusion, which addresses a global analysis of input images, in this study, an analysis of multi-temporal volumes has been carried out, according to the specific local content.

5 Conclusions

Through this work a fusion algorithm supported by the color has been developed, providing the physician with a concrete support in the analysis of a large amount of images. With this method, a complete view has been obtained, showing detail enhancement and high information content preservation.

A first study on synthetic images has allowed defining the best associations between images and RGB channels, where the importance of associating the image with a high information content to the green channel has been pointed out.

The application of the algorithm on the images of the triphasic liver has emphasized the advantage of using the color to interpret the texture of the liver and tumor since the gray levels can fool the eye. The need to perform a processing of images to highlight the pathology with respect to the parenchyma has been demonstrated as well.

References

1. Baum, K.G., Helguera, M., Hornak, J.P., Kerekes, J.P., Montag, E.D., Unlu, M.Z., Feiglin, D.H., Krol, A.: Techniques for fusion of multimodal images: application to breast imaging. In: 2006 IEEE International Conference on Image Processing. IEEE (2006)
2. Goshtasby, A.A., Nikolov, S.: Image fusion: advances in the state of the art. Information Fusion **8**(2), 114–118 (2007)
3. Bedi, S., Jyoti, A., Pankaj, A.: Image fusion techniques and quality assessment parameters for clinical diagnosis: A Review. International Journal of Advanced Research in Computer and Communication Engineering **2**(2), 2319–5940 (2013)
4. James, A.P., Dasarathy, B.V.: Medical image fusion: A survey of the state of the art. Information Fusion **19**, 4–19 (2014)

5. Pujol, A., Chen, L.: Color quantization for image processing using self information. In: 2007 6th International Conference on Information, Communications & Signal Processing. IEEE (2007)
6. Wyszecki, G., Stiles, W.S.: Color science. Wiley, New York (1982)
7. Banu, S., Sattar, S.A.: The comparative study on color Image segmentation Algorithm. International Journal of Engineering Research an Applications **2**(4), 1277–1281 (2012)
8. Paschos, G.: Perceptually uniform color spaces for color texture analysis: an empirical evaluation. IEEE Transactions on Image Processing **10**(6), 932–937 (2001)
9. Kim, A.-R., Kim, H.-s., Park, S.-o.: Measuring of the perceptibility and acceptability in various color quality measures. Journal of the Optical Society of Korea **15**(3), 310–317 (2011)
10. Luo, M.R., Cui, G., Rigg, B.: The development of the CIE 2000 colour-difference formula: CIEDE2000. Color Research & Application **26**(5), 340–350 (2001)
11. Joel Gibson, R.: Spiral CT of the Liver: is Biphasic or Triphasic Scanning the Routine in your Department? In: Advance for Imaging & Radiation Oncology (2010)
12. Tarantino, L., Sordelli, I., Nocera, V., Piscopo, A., Ripa, C., Parmeggiani, D., Sperlongano, P.: Ablation of large HCCs using a new saline-enhanced expandable radiofrequency device. Journal of ultrasound **12**(2), 69–74 (2009)
13. van Leeuwen, M.S., Noordzij, J., Feldberg, M., Hennipman, A.H., Doornewaard, H.: Focal liver lesions: characterization with triphasic spiral CT. Radiology **201**(2), 327–336 (1996)
14. Choi, B., Lee, H., Han, J., Choi, D., Seo, J.B., Han, M.: Detection of hypervascular nodular hepatocellular carcinomas: value of triphasic helical CT compared with iodized-oil CT. AJR. American Journal of Roentgenology **168**(1), 219–224 (1997)
15. Rattanapitak, W., Udomhunsakul, S.: Comparative efficiency of color models for multi-focus color image fusion. Hong Kong (2010)
16. Tsagaris, V., Anastassopoulos, V.: Multispectral image fusion for improved RGB representation based on perceptual attributes. International Journal of Remote Sensing **26**(15), 3241–3254 (2005)
17. Dellepiane, S.G., Angiati, E.: A new method for cross-normalization and multitemporal visualization of SAR images for the detection of flooded areas. IEEE Transactions on Geoscience and Remote Sensing **50**(7), 2765–2779 (2012)